

Analysis of the Factors Contributing to Fatigue in the Cables of Cable-Stayed Bridges

Análisis de los factores que contribuyen a la fatiga de los cables en los puentes atirantados

Miguel A. Astiz ^{a,b}

^(a) Carlos Fernández Casado S.L., Orense 10, 28020 Madrid, Spain

^(b) Technical University of Madrid (UPM), School of Civil Engineering

Recibido el 13 de enero de 2021; aceptado el 7 de mayo de 2021

ABSTRACT

The safety of cable-stayed bridges is mainly relying on the cables and the possible fatigue of these cables has been a concern among designers and researchers for a long time. The main purpose of this paper is to analyze the relative importance of all the factors which may induce fatigue in the cables: static and dynamic effects of live load, pavement roughness, parametric excitation, aerodynamic pressure from traffic, vortex shedding and buffeting. These effects have been evaluated for a wide range of cable-stayed and extradosed bridges which cover most of the present applications of this technology.

This study has shown that the present cable technology and the design rules which are applied nowadays prevent fatigue in the cables. There is room for improvement, thus reducing the cost of the cables but such reduction should consider the conjunction of some of the factors which have been considered in this study, especially the dynamic effects of service loads and vortex shedding.

KEYWORDS: Cables, stays, cable-stayed bridges, fatigue, live load, wind.

© 2021 Asociación Española de Ingeniería Estructural (ACHE). Published by Cinter Divulgación Técnica S.L. All rights reserved.

RESUMEN

La seguridad de los puentes atirantados está basada principalmente en la resistencia de los cables y la posible fatiga de estos elementos ha sido una fuente de preocupación para proyectistas e investigadores. El propósito principal de este artículo consiste en el análisis de la importancia relativa de todos los factores que pueden inducir fatiga en los cables: los efectos estáticos y dinámicos de las cargas de servicio, la rugosidad del pavimento, la excitación paramétrica, la presión aerodinámica del tráfico, el desprendimiento de torbellinos o el efecto de las ráfagas. Estos efectos han sido evaluados para un rango amplio de puentes atirantados y extradosados que cubre la mayor parte de las aplicaciones actuales de esta tecnología.

Este estudio ha demostrado que la tecnología actual de cables y las reglas de proyecto que se aplican a día de hoy evitan la aparición de fenómenos de fatiga en los cables. Hay margen de mejora con lo que se conseguiría una reducción del coste global de los cables pero esta reducción debe conseguirse a través de considerar la conjunción de los factores que han sido contemplados en este estudio, especialmente los efectos dinámicos de las cargas de servicio y el desprendimiento de torbellinos.

PALABRAS CLAVE: Cables, tirantes, puentes atirantados, fatiga, cargas de servicio, viento.

© 2021 Asociación Española de Ingeniería Estructural (ACHE). Publicado por Cinter Divulgación Técnica S.L. Todos los derechos reservados.

1. INTRODUCTION

Fatigue and corrosion in the cables have very soon been found to be one of the key problems in the durability and

maintenance of cable-stayed bridges. Many such bridges suffered partial fractures in some of their stays which derived into complex repairs or in the substitution of cables [1-6]. Many other unreported cable replacements have been or are going to be accomplished in cable-stayed bridges around the world since the first generation of such bridges, which

* Persona de contacto / Corresponding author.
Correo-e / email: maastiz@cfcsl.com (Miguel Ángel Astiz)

were built in the sixties and seventies are already about fifty years old.

The cause of cable deterioration is not only fatigue but also corrosion or the combined effect of fatigue and corrosion. Nevertheless as the present paper will mainly focus on the design of new bridges and present day technology for cable stays almost precludes corrosion, this paper will concentrate on design rules against fatigue for cable stays. Then other phenomena related with the long term behavior of materials such as ageing, creep and shrinkage, crack propagation are not considered in this paper.

Although fatigue is generally thought as being caused by live load, some early studies focused on wind related fatigue crack propagation [7]. Nevertheless it is nowadays generally admitted that fatigue is produced by the combination of a great number of causes which can be classified in two groups since it may originally be caused either by live load or by wind [8]. Live load may induce stress variations in the cables either through static application of the loads, or through the dynamic response of the bridge under the moving loads or through parametric excitation of the cables. Wind may also generate stress variations in the cables through a series of static and aeroelastic mechanisms such as vortex-shedding, buffeting and galloping. Then fatigue is the result of superposing a number of very different phenomena whose relative importance is not well defined.

Design codes have historically tried to simplify the fatigue process by choosing a governing load to take into account in the design against fatigue and to apply convenient safety coefficients to cover the effect of other actions. This governing load is supposed to be the static effect of a specific live load especially defined for fatigue analysis.

The strength against fatigue is generally expressed in terms of the well-known S-N, or Wöhler, curves which relate the stress amplitude with the number of cycles in a test performed with constant amplitude. In these curves a fatigue limit is defined as the value which would correspond to a theoretical infinite fatigue life (usually taken as $100 \cdot 10^6$ cycles). Although such curves are different depending on the magnitude being represented (experimental values or lower bound for design) they suggest two possible design philosophies which are defined in many international codes [8-15]: design to maintain stress variations under a safe fatigue limit or using the S-N curves (obviously modified for design) and Palmgren-Miner rule to compute fatigue material damage thus reaching a more adjusted design. In this context great advances have been performed in cable technology in order to reduce fatigue problems: cable concentrators, cable dampers, cable protection against external damage (corrosion, vandalism, fire); some of these means do have a positive effect on fatigue endurance although this effect may not be reflected in the laboratory tests.

In the context of Eurocodes [9-11], five fatigue load models are defined for highway traffic. Some of them are defined to be applied statically to compute the stress range while others are aimed at permitting the determination of the fatigue spectrum. The standard fatigue strength curve is defined as bilinear (1:4 and 1:6 slopes) in a log-log plot with a strength range of 160 MPa for $2 \cdot 10^6$ cycles in the most frequent case of bundles of parallel strands. The fatigue threshold is not defined although it is usually associated to 10^8 cycles; from the

previously defined bilinear curve this limit would be 83 MPa. Fatigue tests are defined as in the generally accepted *fib* document [12] for a maximum stress of 0.45 GUTS and a stress variation of 200 MPa. If cable stays are supposed to be designed as safe life (effective during the entire life time without maintenance) and with high consequences of an eventual failure, the resultant partial factor would be 1.35. Then the design stress variation is $160/1.35 = 118$ MPa for $2 \cdot 10^6$ cycles (or 62 MPa for $1 \cdot 10^8$ cycles). Consequently the actual safety factor with respect to the measured strength is $200/118 = 1.69$ which is supposed to take into account the uncertainty about the actual fatigue strength as well as the presence of other actions contributing to fatigue.

On the other side, the AASHTO Design Specifications [13] two fatigue limit states: Fatigue I (load factor 1.75) corresponds to design for infinite fatigue life design and Fatigue II (load factor 0.80) corresponds to finite life design. In both cases the load to be applied corresponds to a single 320 kN truck with a dynamic allowance. Cables of cable-stayed bridges are not considered in this code.

Design against fatigue in the cables is specifically treated in the PTI Recommendations [14]. With respect to testing of stay cable assemblies, the main difference between *fib* [8] and PTI is that in PTI two tests have to be performed with a maximum stress of 0.45 GUTS and one test has to be performed with a maximum stress of 0.55 GUTS. The stress range for the fatigue tests is 200 MPa for *fib* while it is 159 MPa or 121 MPa (for an upper bound stress of 0.45 or 0.55 GUTS respectively) for PTI. The design limit for $2 \cdot 10^6$ cycles is equal to the testing range minus 69 MPa in the case of strands. Fatigue design is performed by applying a single fatigue truck (as defined by AASHTO) in each traffic direction multiplied by two coefficients whose overall result is a 5% increase over the nominal value. The design methodology for fatigue considers two possible situations. The first one corresponds to the case where the design stress variation is lower than the factored fatigue limit which is set to be 55 MPa for parallel strands; in this case there is no fatigue and no further check has to be performed. The second one requires computing the fatigue strength for constant amplitude stress variation as a function of the number of load cycles which are foreseen to be applied during the bridge service life; this value is reduced by a 0.5 factor and compared to the design stress variation. In any case only axial force variations are taken into account in the fatigue checks.

Previous information shows that the European approach to the design of the cables against fatigue and the corresponding American approach are not consistent. This fact leads to not consistent design specifications to be applied to specific bridges since it is frequent to see that the client specifies fatigue tests according to *fib*, loading according to Eurocodes and checks according to PTI. SETRA Recommendations [8] propose a combination of both approaches by setting the European FLM3 fatigue vehicle as the load to compute the applied stress variation and by defining the fatigue limit for design from a bilinear SN curve as in EC1993-1-11 [11]. The stress variation corresponding to $2 \cdot 10^6$ cycles is the test value (200 MPa) divided by a partial safety factor of 1.5; the resulting value is $200/1.5 = 133$ MPa and a fatigue limit is defined for $100 \cdot 10^6$ cycles as 0.52 times the test value. As it is required that the bridge should withstand $100 \cdot 10^6$ passages of the FLM3 vehicle

of the Eurocode, the fatigue check reduces to verify that the FLM3 vehicle may cause a stress variation in the cables smaller than 70 MPa. This check is comparable although not the same as the PTI check which defines a maximum stress variation of 55 MPa for a 320 kN vehicle while the weight of the FLM3 vehicle is 480 kN. The Spanish Recommendations for cable stays [15], similar to SETRA, also require that the stress variations due to wind should be smaller than the previously defined fatigue limit.

As all the previously mentioned codes and recommendations are based on a fatigue check consisting in computing the stress variations due to vertical live loads without taking into account other effects, the purpose of this paper is to verify what is the relative importance of all the factors which may induce fatigue in the cables and to try to check the validity of the present approach to fatigue design. The importance of this issue may be shown by the number of studies about FRP cables to be applied to very long span cable-stayed bridges which consider all the fatigue prone factors in the design of such cables [16-19].

This study is to be performed over a representative range of cable-stayed bridges. This range includes basically four types of bridges: cable-stayed bridges with concrete deck (with cables anchored at the edges and at the center of the deck) and with a composite deck and extradosed bridges with concrete deck. These cases do not cover all the possible types of cable-stayed bridges since steel deck is not considered and the composite deck for extradosed bridges is not considered either. Nevertheless the bridge types which are considered represent a very important part of all the cable-stayed bridges which are being built nowadays. Again, as the aim of this paper is to clarify the importance of a number of effects in the design of bridges, only current technology for cables is to be considered.

The paper is divided in three sections. The first one describes the bridge models which have been developed to back the study. The other two sections correspond to the two main loads which may cause fatigue in the cables: live load and wind. In any case fatigue analysis is restricted to the cables only. Fatigue in the anchorages is not studied here because of the high variety of shapes and materials and the purpose of this paper is to present conclusions which could be applicable to most design cases and which, consequently, could be useful to designers.

2. BRIDGE CASES AND MODELS

As previously explained, four different bridge cases are being considered. In all of them the scheme consists of one main span and two approach spans (all of them cable-stayed) with two pylons. The case of one main span with one back span, which is quite frequent, is not considered since it could be reduced to the symmetric scheme in terms of relative stiffness between deck and cables. Three span lengths shall be considered for each bridge type; these span lengths do not cover the full range of span lengths which are being built nowadays but they try to cover the most reasonable range within each bridge type; especially in the case of cable-stayed bridges with a composite deck, it is admitted that this option may be economi-

cally valid for up to 800 m span [20] but this study is being restricted to commonly built solutions. Then the cases which are studied are (figure 1):

- a) Cable-stayed bridges with a concrete deck (CS-CONC); span lengths: 200, 300, 400 m.
- b) Cable-stayed bridges with a composite deck (CS-COMP); span lengths: 400, 500, 600 m.
- c) Extradosed bridges with a concrete deck (EX-CONC); span lengths: 100, 150, 200 m.
- d) Cable-stayed bridges with a concrete deck and anchored at the center of deck (CC-CONC); span lengths: 200, 300, 400 m.

The lateral span length is half the main span and the excess in flexibility which is associated to this ratio between the lateral and main spans is usually compensated by some intermediate piers in the lateral spans; in this study only one is being considered. In the first three groups only a ladder-type deck (two edge girders with cross beams) has been considered since the deck is supposed to be supported by cable anchorages at both edges. The case of a closed box for the deck and a central plane of cable stays is being considered for completeness although it is supposed that this different configuration may have only a small influence in the fatigue conditions of the cables.

For each of the twelve cases which are being studied a structural model made of beam and truss elements has been built. The geometric characteristics of each bridge (height and layout of towers, distance between cable anchorages, deck depth) have been chosen as the average values among the actually built bridges which fit into each category. In the case of the layout of the towers different schemes have been chosen for each type of bridge: H-shaped with two cross beams for cable-stayed bridges of middle size (concrete deck), inverted Y towers for the long span cable-stayed bridges (composite deck), H-shaped towers with a single cross beam for the extradosed bridges and a single vertical stem for the bridges with a central plane of cables. Constant depth decks have been chosen for the cable-stayed bridges while a variable depth deck has been defined for the extradosed bridges. Cables have been designed on the basis of a maximum service stress of 0.45 GUTS for the cable-stayed schemes and 0.60 GUTS for the extradosed bridges with no consideration for fatigue constraints. The four types of bridges along with a perspective view of their corresponding models have been represented in figure 1.

Two general parameters have been studied for these bridges which are related to their static and dynamic behavior. To characterize the static behavior of each bridge in relation with the cables a uniformly distributed load has been applied on the main span and the resulting deflection, v_{total} , at mid span has been compared to the deflection at the same point if the deck was not supported by cables, v_{deck} . By supposing that the stiffness of the bridge is the sum of the stiffness of the deck and of the cable system it may be deduced that the participation of the cables in the total stiffness of the bridge is

$$\frac{k_{cables}}{k_{total}} = 1 - \frac{k_{deck}}{k_{total}} = 1 - \frac{v_{total}}{v_{deck}} \quad (1)$$

where K stands for stiffness, which is the inverse of flexibility. Resulting values for the different cases have been plotted on

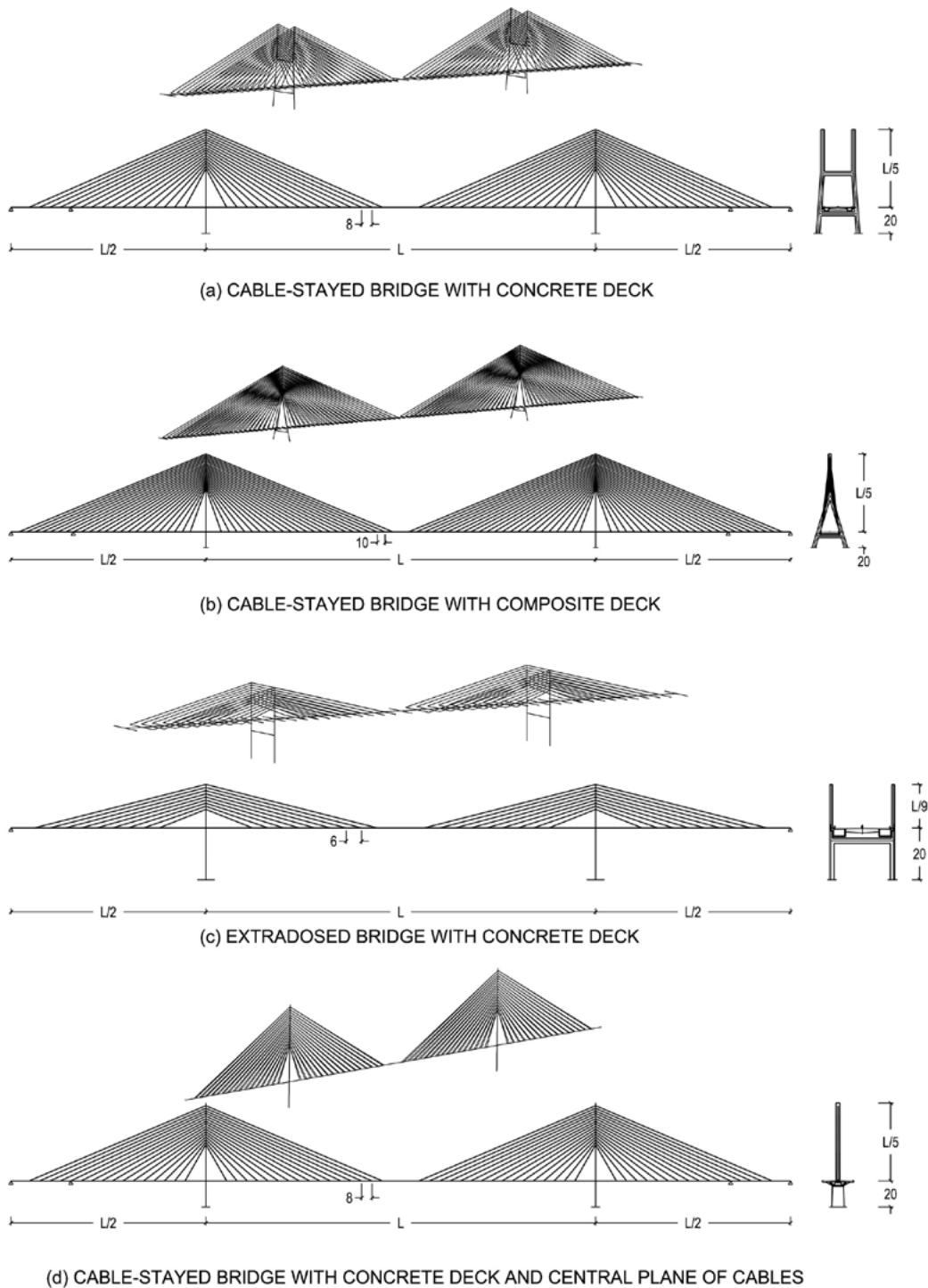


Figure 1. Layout and models for: a) Cable-stayed bridges with concrete deck (CS-CONC), b) Cable-stayed bridges with composite deck (CS-COMP), c) Extradosed bridges with a concrete deck (EX-CONC) and d) Cable-stayed bridges with concrete deck and central plane of cables (CC-CONC).

figure 2. In this figure it can be appreciated that, as it is well known, the stiffness of the cable-stayed bridges almost completely relies on the cable system since the deck depth to span ratio is smaller than 1/100 for the intermediate spans and smaller than 1/200 for the longer spans; this is not exactly true for the cases with a single plane of cables (and a closed box deck) since the corresponding deck is stiffer and the influence of a

concentrated load on the cables is smaller (because this load is shared among a larger number of cables) In the case of extradosed bridges, the deck and cables participation in total stiffness of the bridge is similar, around 50%; this is mainly due to the fact that the deck depth to span ranges between 1/30 and 1/50 which are values closer to those of a continuous girder bridge. This means, apparently, that the cable system would

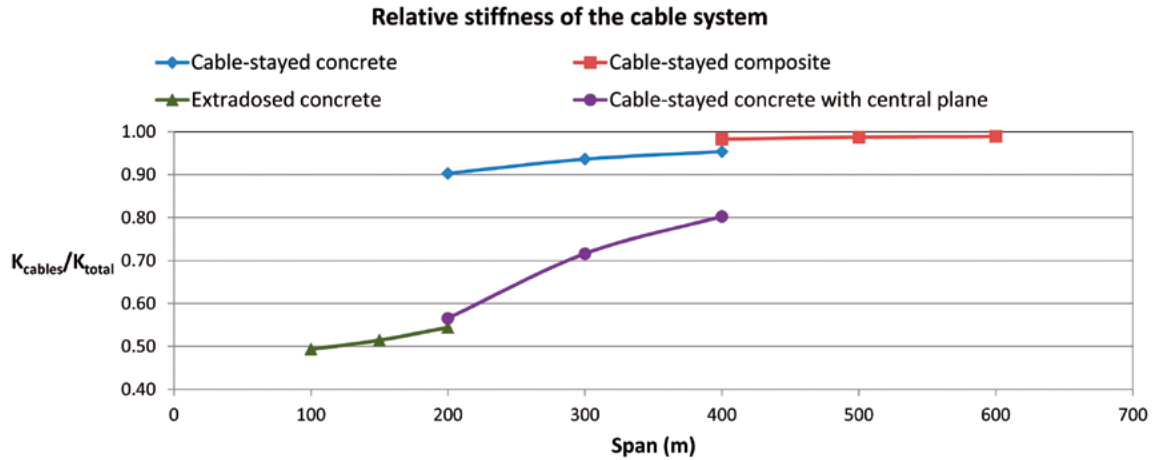


Figure 2. Relative stiffness of cable system for the selected bridge schemes.

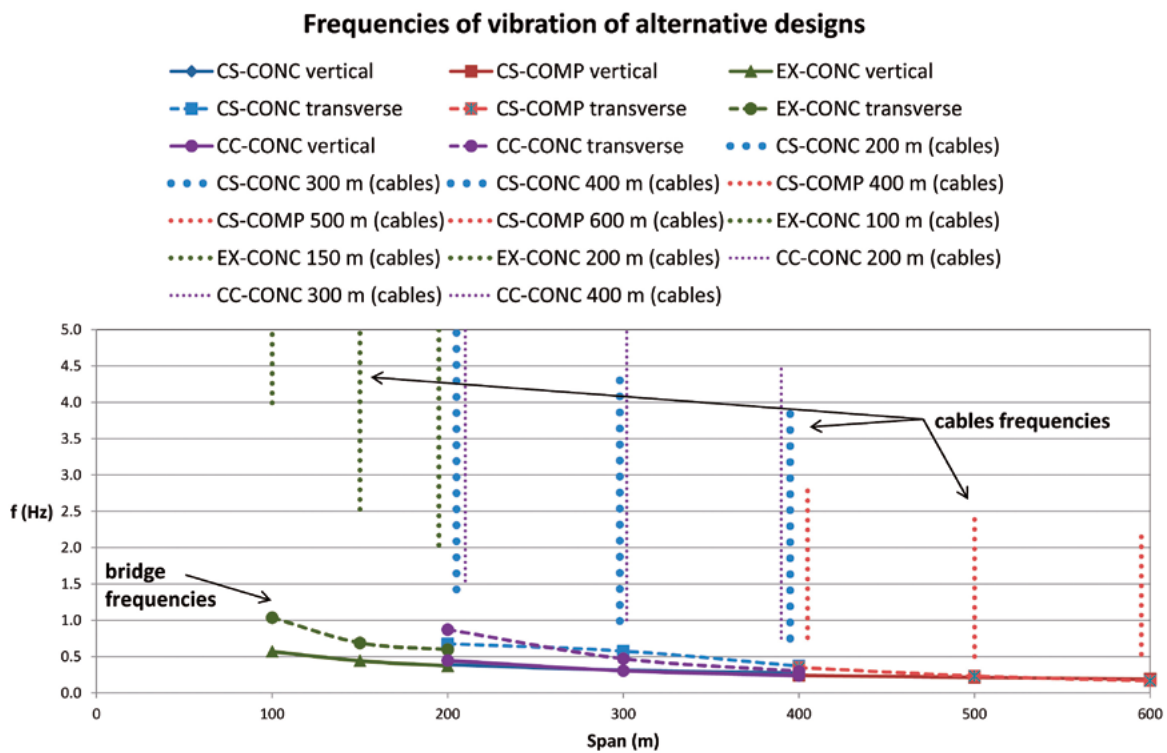


Figure 3. First vibration frequencies (vertical and transverse) for the different bridge schemes and for the cables.

absorb larger forces under service loads for the cable-stayed bridges than for extradosed bridges. This argument may be somewhat misleading as it will be shown later.

The dynamic behavior of the different bridge cases is mainly characterized by the vibration frequencies. Figure 3 shows the variation of the first frequencies (vertical and transverse) for each type of bridge as a function of the span length. It must be noted that there is certain continuity between the different bridge schemes which shows that the span length is the governing parameter with respect to vibration frequency, independently of the deck mass or the cable system configuration. In this respect, the comparison between the concrete bridges with alternative suspension systems (at edges or at the deck axis) and the same range of span lengths shows very

similar results. It is worth mentioning that in all cases the fundamental frequency has not been shown in figure 3 since in most cases it corresponds to a longitudinal movement of the deck and the pylons combined with an antisymmetric vertical movement of the deck; this frequency is very much dependent on the modeling of the deck supports and constraints which are defined on the basis of temperatures and other loads such as seismic and braking. Nevertheless this fundamental mode will become relevant in some cases as it will be shown later.

But the main purpose of this figure is to compare the bridge frequencies to the cables frequencies (only the fundamental cable frequencies have been plotted on figure 3). The vertical lines represent the range of variation of the fundamental cable

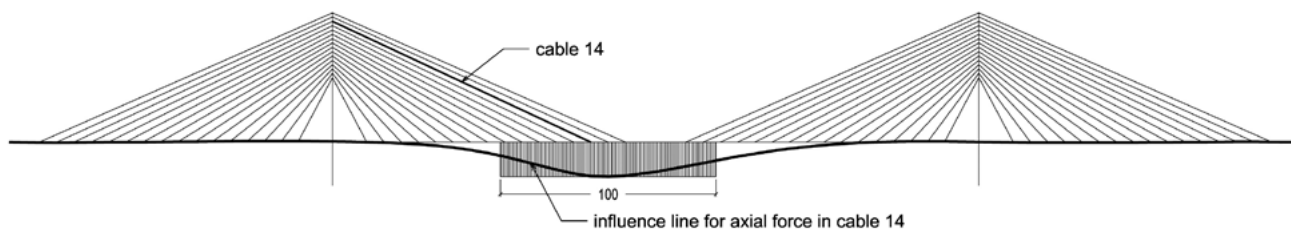


Figure 4. Influence line of axial force in cable 14 for the case of a cable stayed bridge with 300 m span and a concrete deck (CS-CONC 300 m).

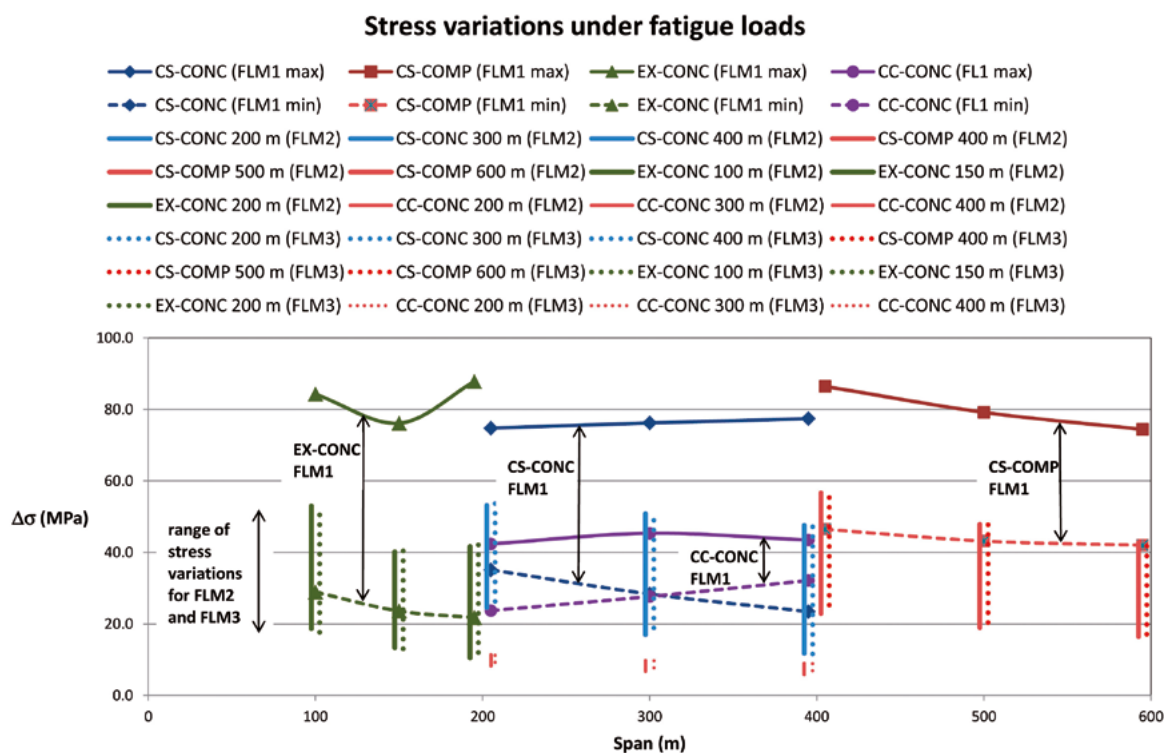


Figure 5. Stress variations for the three bridge classes and for the three fatigue load models (FLM1, FLM2 and FLM3).

frequencies for the different cables of the bridge; the shortest cables exhibit greater frequencies than the longest cables. The interest in comparing the bridge and the cables frequencies consist in investigating the possible coupling of bridge and cable vibrations. According to the present results this coincidence is more likely to occur for longer spans; it is very unlikely for extradosed bridges. In the case of cable-stayed bridges, figure 3 indicates no coincidence between the bridge and the cables frequencies but this happens with the particular models and designs which have been proposed here; different designs may drive to coincidences as it has happened historically. It has also to be pointed out that figure 3 only compares the first frequencies of the bridge and the cables but coincidence may occur between higher frequencies of different order for the bridge and the cables. This dynamic interference between the bridge and the cables will be studied later.

3. FATIGUE DUE TO LIVE LOAD

3.1. Static analysis

Static analysis is the standard method which is used in the design of the bridge. As previously mentioned, EN1991-2 [9] provides three fatigue load models named FLM1, FLM2 and FLM3 for defining maximum and minimum stresses due to different loads in the bridge (two more models are provided in relation to fatigue spectra). Fatigue load model FLM1 is a fraction of the standard LM1 model for static analysis of bridges (uniformly distributed load of 2.7 kN/m² and a 2 axle vehicle of 420 kN, both of them being applied on a single lane) while FLM2 and FLM3 consist of different vehicles with total weights ranging between 280 and 630 kN which are supposed to be representa-

tive of actual traffic (only a single vehicle is applied at a time on the full bridge for FLM2 and two vehicles for FLM3 although the second vehicle is only 30% of the first one).

An important fact to be taken into account is that any concentrated load applied on a cable-stayed bridge is distributed among many cables by the stiffening girder; consequently a distributed load which is applied along the whole bridge will have a more important effect on the cables than any concentrated load. This fact may be observed in figure 4 where the influence line for the axial force in one cable is shown in a case which has been taken as an example; this figure demonstrates that a uniformly distributed load may represent a very significant contribution to the axial force in any single cable. As shown in the figure, the effect of 2.7 kN/m² would be equivalent, for a 3.0 m wide lane to a concentrated load of $2.7 \times 3.0 \times 100 = 810$ kN which is heavier than any of the vehicles which are proposed to check fatigue conditions. The consequence is that fatigue load model 1 (FLM1) is conservative in the case of the cables as it is already recognized in its definition [9].

The effect of FLM1 is shown on figure 5 by two lines for each class of bridges: the top line corresponds to the maximum stress variation (usually corresponding to the shortest cable) and the lower line corresponds to the minimum stress variation (usually corresponding to one of the longest cables). In the same figure the vertical lines show the range of stress variations corresponding to FLM2 (continuous vertical lines) and to FLM3 (discontinuous vertical lines).

These results show that the stress variations corresponding to FLM2 and FLM3 are very similar and that they are generally below the fatigue limit when cables are designed on the basis of the maximum service stress being smaller than 0.45 GUTS for cable-stayed schemes and smaller than 0.60 GUTS for extradosed schemes. The reason for the equivalence between FLM2 and FLM3 results is that the heaviest vehicle has similar weight in both cases (a vehicle of 630 kN for FLM2 and a vehicle of 480 kN plus another one of 144 kN totalling 624 kN for FLM3)

Another important result is that the stress variations corresponding to the extradosed scheme are comparable to those of the cable-stayed schemes. Although this result may not be considered as general since it may depend on the design of the deck and on the maximum allowed service stress in the cables, it is important to point out that the trend to design the cables of the extradosed bridges with a higher service stress has to be first justified by an analysis if the stress variations under fatigue loads are smaller than a certain limit as proposed by the SET-RA Recommendations [8].

By comparing the results of the two concrete alternatives (deck anchored at the edges or at the center) it must also be noted that the deck stiffness plays a very important role since a stiffer deck distributes the fatigue load among a larger number of cables thus reducing the stress variations in the cables.

3.2. Dynamic effects of service loads

As all the fatigue load models of EN1991-2 include dynamic load amplification, previous static analysis is deemed to be sufficient for checking fatigue. Nevertheless, most bridge load standards are written for small to medium span bridges. Analyses and experimental checks have generally been performed

for such bridges [21,22]. Cable-stayed bridges, which are more flexible, may exhibit a different dynamic behavior and, as the purpose of the present paper is to compare all possible sources of fatigue, a dynamic check is being presented.

In a first phase, pavement is supposed to be perfect and no truck oscillations are considered. Then the analysis just consists in computing the effect of some particular moving loads. As the shape of the influence line of cable loads (figure 4) shows a long and smooth maximum, analysis of the maximum effect due to different vehicles may reduce to analyzing only the heavier vehicle. Then only the 630 kN lorry of the Eurocode FLM2 has been considered. The loads of the 5 axles of this vehicle have been moved at different velocities along one of the outside lanes of the bridge in order to obtain the maximum load variation in every cable. Although fatigue analysis would require a more detailed analysis to take into account damage calculation on the basis of the Palmgren-Miner rule and the rainflow cycle counting algorithm on a more realistic traffic model (such as the Eurocode FLM4 or FLM5) dynamic analyses have been performed to compute maximum stress variations (as it is done with static analyses with the FLM2 model) and to evaluate the importance of dynamic effects.

Results do not show a smooth variation since some local resonance effects may appear but it has been observed that within every bridge scheme they are quite consistent. Then it seems that the response of these bridges in terms of axial loads variations are relatively independent of span length and other parameters such as the relative rigidity between cables and deck, the mass of the deck, the distance between cable anchorages in the deck or the angle between the cables and the deck may be more relevant. Then results have been represented as mean values among all the span lengths of the dynamic amplification factor (DAF) for each scheme as in figure 6. In this diagram there are two curves for each bridge type: one corresponds to the maximum stress variation among all the cables of the main span of the bridge and the other one corresponds to the minimum value (maxima usually correspond to the shortest cables and minima correspond to the longest cables). These extreme values are actually the mean of the corresponding extreme values for the three span lengths which are being considered in each bridge scheme.

Although these results may not be taken as absolutely general since they depend on a number of factors as previously mentioned and they also may depend on the type of discretization and modelling which has been used in the calculations, they indicate important differences between the different bridge schemes. From the point of view of the main purpose of this article, it is worth to mention that the dynamic allowance which has been foreseen in the Eurocode is an impact factor of 1.2 for shear (the force which may be assimilated to cable force)[23]; only span lengths smaller than 200 m have been considered in the calibration of the Eurocode. Present results show dynamic amplification factors which are significantly greater than this value (up to 30% increase). This result indicates that the fatigue check for the cables of cable-stayed and extradosed bridges cannot be limited to computing the static variation of cable forces under FLM3 and FLM4; at least a dynamic analysis similar to what has been done here is to be performed.

But the movement of the loads is not the only cause for a dynamic effect on the cable forces. Pavement irregularities

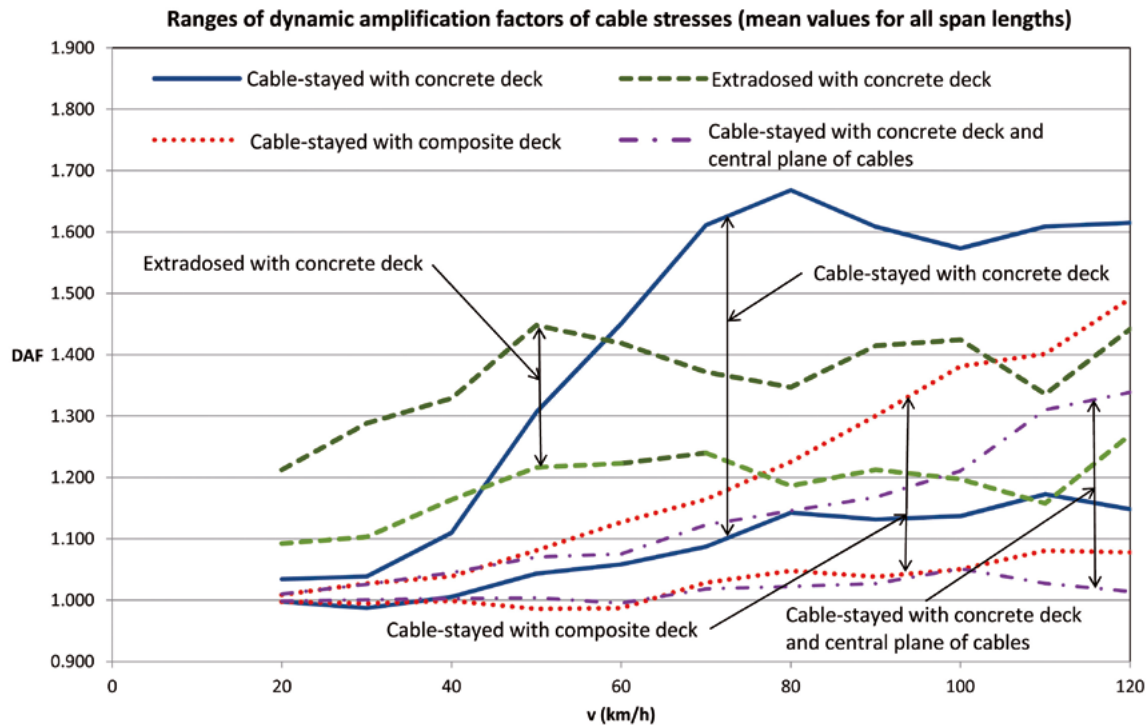


Figure 6. Maximum and minimum values of the mean dynamic amplification factor of cable stresses among all the spans within the same bridge type.

may also cause oscillations in the vehicles and, as a consequence, some variation of the applied loads. To study this effect, pavement irregularities can be modelled by means of a power spectral density function which takes into account not only the longitudinal variations of pavement height but also the transverse variations and the stiffness and damping of the suspension system of the vehicles [24, 25]. In the case of long span cable-supported bridges, and on the basis of the already mentioned shape of the line of influence of cable axial force, only the total vehicle applied load will be relevant; then it has to be expected that pavement irregularities will only have a marginal influence on cable forces.

Numerical simulation of pavement roughness is performed by means of its power spectral density, which is defined in ISO8608 [26] or in the Eurocode 1, Annex B [9] as

$$G(n) = G(n_0) \left(\frac{n}{n_0} \right)^{-2} \quad (2)$$

where $G(n)$ is the power spectral density, n is the spatial frequency (measured in cycles/m) and n_0 is a reference frequency which is taken to be 0.1 cycle/m. In this case the relevant value of $G(n_0)$ is $64 \cdot 10^{-6} \text{ m}^3$ for a good quality pavement (ISO8608 defines 5 categories of pavement ranging from very good to very poor). In cable supported bridges it is supposed that the quality of pavement is superior but it may turn out to be just good after a few years. For medium quality pavements $G(n_0)$ would be 4 times larger and for poor quality pavements it would be 16 times larger; consequently pavement roughness would be 2 and 4 times larger respectively than the roughness corresponding to a good quality pavement. The simulation of two parallel profiles is made by supposing that pavement is ho-

mogeneous and isotropic [24, 25] and 2048 frequencies have been considered between 0.01 and 10 m^{-1} . Road irregularities are sampled every 0.01 s, corresponding to 0.28 m for a vehicle velocity of 100 km/h.

The 630 kN FLM2 vehicle is modelled by a system of springs and dashpots connected by rigid beam elements as shown on figure 7. The different parameters of this model are summarized on table 1; these values are derived from its weights and dimensions, from the model used by Chen et al. [27] and from the well known fact that main vertical frequencies for trucks are around 3 Hz for suspensions and 9 Hz for tires [28].

TABLE 1. Mechanical characteristics of the 630 kN FLM2 vehicle

Mass of body (t)	59.0
Mass of wheels/axles (M_{w_i}) (t)	0.49; 0.81; 0.65; 0.65; 0.65
Height of center of gravity (m)	1.7
Moment of inertia I_x of body (tm^2)	19.7
Moment of inertia I_y of body (tm^2)	752
Moment of inertia I_z of body (tm^2)	752
Horizontal stiffness of tires ($k_{t_{hi}}$) (kN/m)	6500; 6500; 6500; 6500; 6500
Vertical stiffness of tires ($k_{t_{vi}}$) (kN/m)	14700; 29300; 19600; 19600; 19600
Horizontal damping of tires ($c_{t_{hi}}$) (kNs/m)	7; 7; 7; 7; 7
Vertical damping of tires ($c_{t_{vi}}$) (kNs/m)	7; 7; 7; 7; 7
Horizontal stiffness of suspensions ($k_{s_{hi}}$) (kN/m)	1500; 1500; 1500; 1500; 1500
Vertical stiffness of suspensions ($k_{s_{vi}}$) (kN/m)	1500; 3000; 2000; 2000; 2000
Horizontal damping of suspensions ($c_{s_{hi}}$) (kNs/m)	22; 22; 22; 22; 22
Vertical damping of suspensions ($c_{s_{vi}}$) (kNs/m)	22; 22; 22; 22; 22

In a first phase this model of the vehicle is set to run along a roughness profile which has been generated numerically as

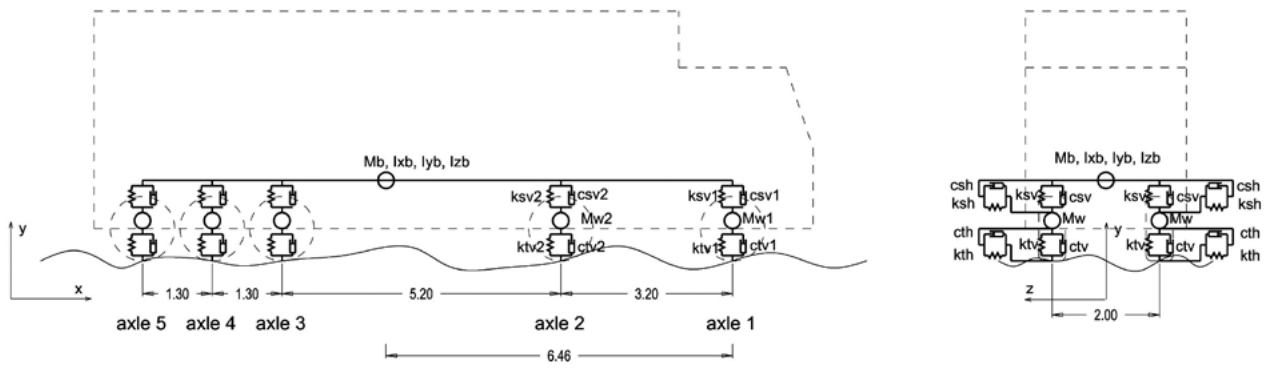


Figure 7. Mechanical model of the 630 kN FLM2 vehicle.

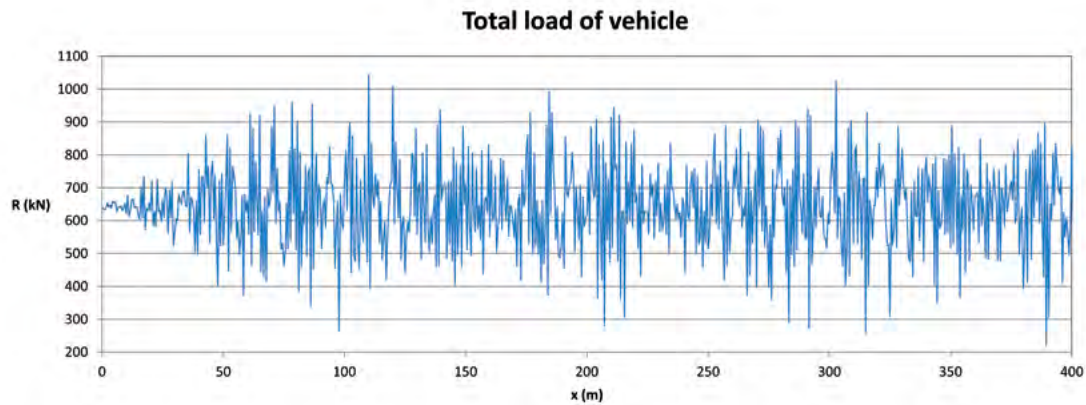


Figure 8. Total load of a 630 kN vehicle running at 100 km/h over a "good quality" pavement.

previously explained. The total reaction, which is the sum of the reactions at the 5 axles (10 wheel units) of the vehicle, is computed as a function of time or distance. In this simulation the velocity of the vehicle has been set at 100 km/h as the most likely velocity of the vehicle. Results, which are shown on figure 8, are somewhat surprising since, for a 630 kN vehicle, total reaction may increase up to 1000 kN; this is a singular peak which may not be relevant but many peaks are observed above 800 kN; this roughly represents a 27% increase of the load, which may be very relevant.

Another interesting result is that a certain periodicity of the peaks may be defined for an 8.3 m distance, which for 100 km/h is equivalent to a time period of 0.3 s, or a frequency of 3.3 Hz. Since this frequency is very different for the fundamental frequencies of cable-supported bridges, no dynamic interaction may be expected between the vehicle vibrations and the bridge vibrations. Consequently, the bridge vibrations, and the corresponding cable load variations, may be studied by just applying the previous vehicle load histories to the bridge model in a step by step analysis. For so doing 128 modes of every bridge model have been considered to cover all possible interactions between the vehicle and the bridge (the frequency corresponding to the 128th mode depends very much on the type of bridge and boundary conditions which have been assumed in each case; for the models which have been considered in the study, the 128th frequency ranges between 5.34 and 31.18

Hz). In any case it has to be pointed out that, depending on the bridge structural model, cable forces may be determined by local modes with very high frequencies; this is the reason why results are shown in a relative format. Dynamic analyses have been performed for all the bridge models with the 7 load histories (similar to that of figure 8). Cable force variations are computed for each load history and the mean of these 7 values is retained as the likely variation of cable force.

Results are summarized in table 2 where they are presented, for each bridge model, as the maximum dynamic amplification factor (DAF) among all the cables of the corresponding model. Although no final conclusions may be derived from these results because they correspond to particular bridge designs, to a single truck load and to a fixed velocity (100 km/h), it seems clear that concrete bridges are more sensible to the vehicles vibrations and that the final DAF's which have been obtained are far beyond the dynamic allowance which has been foreseen in the Eurocode for fatigue load models. The case of the cable-stayed bridge with a single plane of cables is somewhat different because of two reasons: a) the cables are in general less affected by concentrated vehicle loads since the deck by being stiffer distributes the loads among a larger number of cables and b) the heavy vehicle loads are applied on the outside lanes and they are transmitted more directly to a single plane of cables when the anchorages are located along the edges of the deck while they are transmitted to both cable

TABLE 2.
Maximum dynamic amplification factors among all the cables of each bridge ($v=100\text{km/h}$)

Static scheme	Span (m)	DAF for smooth pavement	DAF for rough pavement	DAF increase (%)	Mean DAF increase for each bridge type (%)
Cable-stayed with concrete deck	200	1.603	2.600	62	67
	300	1.683	2.768	64	
	400	1.433	2.492	74	
Cable-stayed with composite deck	400	1.441	1.851	28	30
	500	1.382	1.751	27	
	600	1.320	1.767	34	
Extradosed with concrete deck	100	1.408	4.101	191	182
	150	1.440	4.226	193	
	200	1.424	3.736	162	
Cable-stayed with concrete deck and sigle plane of cables	200	1.119	1.508	35	20
	300	1.226	1.360	11	
	400	1.206	1.376	14	

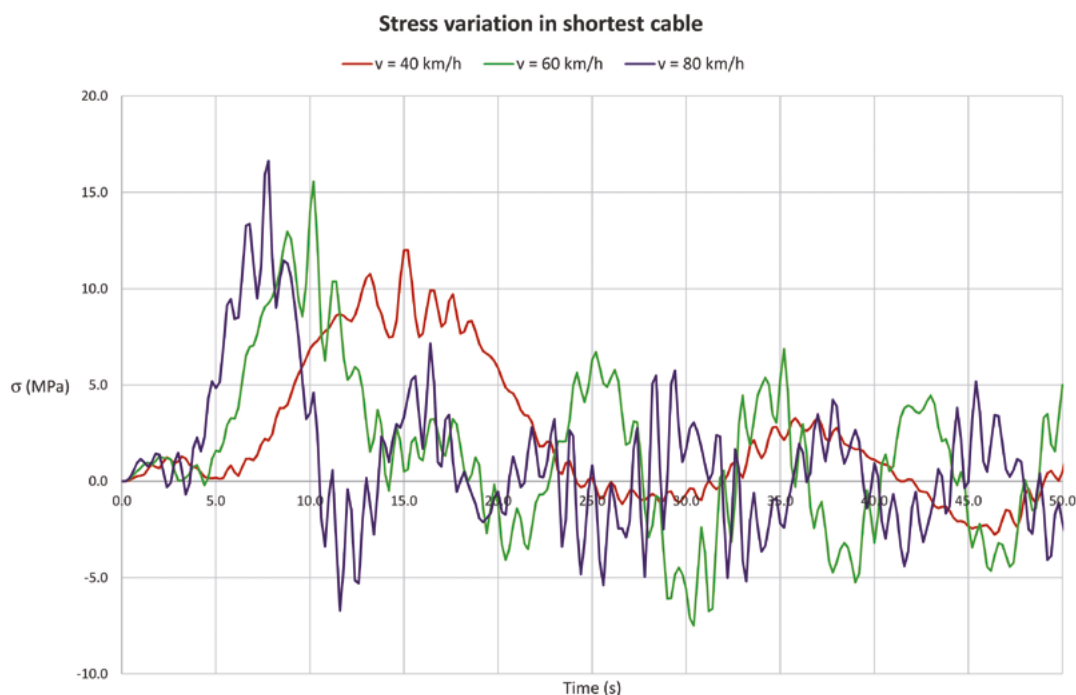


Figure 9. Cable stress variation for the shortest cable of the cable-stayed bridge with a concrete deck and 300 m span under the action of a 630 kN vehicle running at different velocities.

planes when the anchorages are located along the deck axis.

Another interesting result which has been derived from all these dynamic analyses refers to the number of load cycles. Figure 9 shows the variation of cable force in the shortest cable of the cable-stayed bridge with a concrete deck and 300 m span under the 630 kN vehicle travelling on a smooth pavement at different velocities. Apart from the increase of maximum stress which had already be shown on figure 6, it is interesting to see that bridge vibrations are persistent because of the low damping which is typical of cable-supported bridges (a 0.5% value has been assumed in all cases); this fact has already been signaled by other authors [21, 22]. Although

the stress variations which are shown on figure 9 are small in terms of possible fatigue damage, the superposition of several vehicles may bring the stress variations to fatigue prone levels. This kind of studies would require a traffic simulation (through Montecarlo models) and it is unpractical for design purposes but some research in this field would be interesting in order to take into account this effect in the fatigue checks.

3.3. Parametric excitation

Parametric excitation of the cables has been observed in a number of bridges and it has been reported and studied by

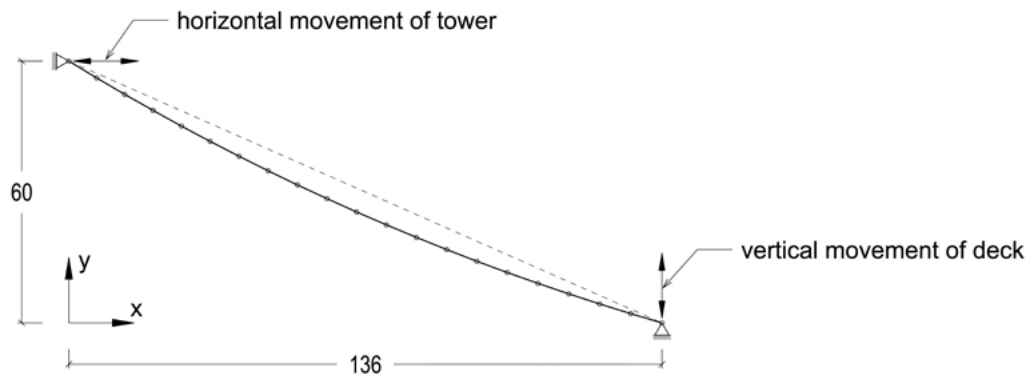


Figure 10. Numerical model of a cable.

many authors [29, 30]. It consists in the lateral (vertical and/or transverse) vibration of the cables due to the movement of the deck (and possibly also of the towers); the movement of the deck may be due either to vertical service loads or to transverse wind loads. If these movements of the deck are persistent (and it has already been shown before that they may be persistent as in figure 9), the movements of some cables may be very relevant if the parameters of these cables fall in the so-called instability zones which are defined as a function of the ratio between the frequencies of the structure and the cable. This is the reason why only some cables may be affected by this phenomenon in a particular bridge.

If the ratio between both frequencies is defined as $\beta=f/2f_c$ where f is the excitation frequency (usually coincident with the bridge frequency) and f_c is the cable frequency, the instability zones are mainly formed around $\beta=1$ ($f=2f_c$, called zone I) and around $\beta=0.5$ ($f=f_c$, called zone II) but depending on the amplitude of the excitation and on cable damping these ratios can move even far from these theoretical values. In practice, a threshold of excitation amplitude may be defined for each cable. The analytical solution of this problem requires forming a non-linear differential equation and trying to find unbounded solutions to it. Although this method may give a good insight to the problem, the check at design phase may be performed by means of a numerical model which may take into account all the circumstances of the problem: actual shape and slope of the cable, longitudinal deformability, direction and variation of the movements at its ends, geometrical non-linearities, damping and even possible bending stiffness. As it would be unpractical to try to consider all these variables, a simple case shall be presented in order to evaluate the importance of parametric excitation in the fatigue of the cable, which is the main purpose of this paper. According to figure 3, the cable-stayed bridge with a concrete deck and 300 m long span is the smallest bridge with a possibility of experiencing parametric excitation; then the longest cable of this bridge is adopted as a case study. The corresponding numerical model is shown on figure 10. The cable is modeled by means of 20 strut elements with no bending stiffness and fixed ends.

The rigorous analysis of the stability of the cable requires going through the following steps:

a) Defining the undeformed length of the cable and building a straight structural model composed of a reasonable number of strut elements (20 in this case).

- b) Submitting the model to the permanent force of the cable. The cable length will be increased up to the theoretical value corresponding to the final geometry of the bridge (as shown in figure 10) but it still will be straight.
- c) Submitting the model to the weight of the cable. The cable will adopt its catenary shape.
- d) Finally, the ends of the cable are submitted to the movements which have been computed in the analysis of the service loads (in this case the fatigue load models). The most relevant displacements are the vertical displacement of the deck and the horizontal (longitudinal) displacement of the tower as shown in figure 10. There is no problem in adding to these displacements the displacements in other directions at both ends.

All these steps have to be accomplished with a program which takes into account geometric non-linear effects since they absolutely condition the behavior of the cables. The most relevant anchorage displacements for the present cable are shown in figure 11, where it may be noted that the vertical movements of the deck are not very important once the vehicle has run through the bridge; the horizontal movements of the tower are more important and, as they damp very slowly, they are responsible for the largest cable force variations. Nevertheless it has also to be noted that the vertical displacements of the deck introduce a small oscillation ($\pm 5\text{mm}$) but with a frequency (1 Hz) which is similar to the fundamental frequency of the cable (0.93 Hz).

When these displacement histories (along with those corresponding to other directions) are applied on the model, the response may be analyzed by looking at cable rotations at the anchorages since these rotations are mainly responsible of stress variations at or close to the anchorages. The stress variation is computed as [8, 15]:

$$\Delta\sigma = 2\beta\Delta\alpha \sqrt{E\sigma_0} \quad (3)$$

where $\Delta\alpha$ is the cable rotation at the anchorage, E is the cable modulus of elasticity, σ_0 is the permanent cable stress and β is a factor which depends on the position and size of the elastomeric ring which is usually set near the anchorage (a value of 0.5 is usually applied for this parameter). It must be noted that in the case of a cable on a deviator (such as saddles or

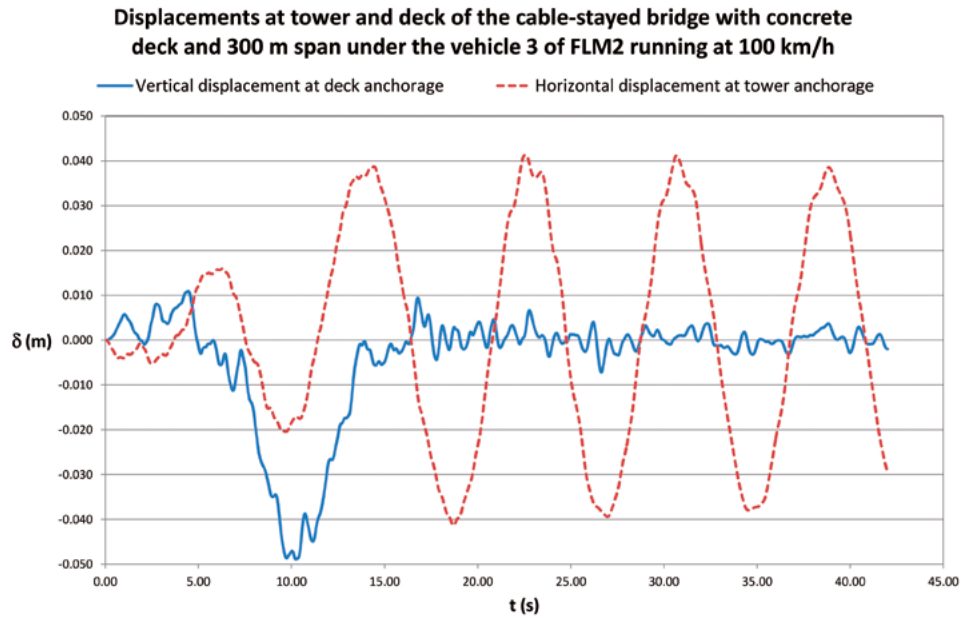


Figure 11. Variation of most relevant displacements at the tower and deck anchorages of the longest cable when the vehicle 3 of FLM2 (630 kN) runs through the cable-stayed bridge with a concrete deck and a 300 m long span at 100 km/h.

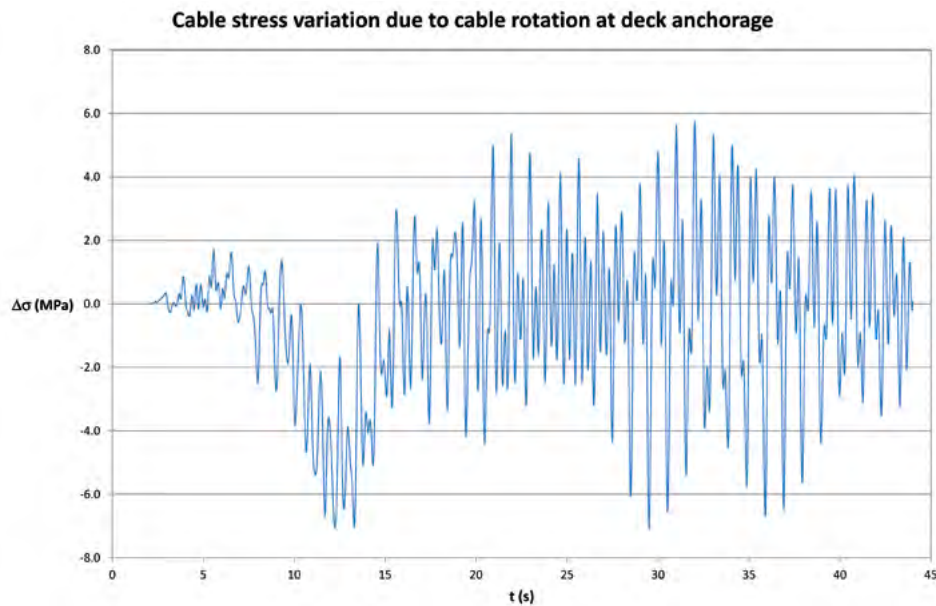


Figure 12. Stress variation due to cable rotation at the deck anchorage of the longest cable when the vehicle 3 of FLM2 (630 kN) runs through the cable-stayed bridge with a concrete deck and a 300 m long span at 100 km/h.

deviators for external prestressing or anchorages including a deviator) equation (3) should be modified to take into account the curvature effect on wire stress. The resulting stress variation which has been derived from the 630 kN vehicle is shown on figure 12. This figure shows relatively low values of stress variations, which had to be expected since the cable and bridge frequencies are not similar, but these values have to be added up to the uniform deformation of the cable due to the same vehicle either static (figure 5) or dynamic (figure 9). The vibration is stable since it shows a tendency to diminish with time. To look for possible instability zones, the same displacement histories have been applied to the cable after multiplying them

by an increasing factor ranging from 2 to 16 and no divergent vibrations have been observed; again, this result is the consequence of the absence of possible resonance effects. In a resonant condition, the situation might be completely different but in this case the concern would not only be fatigue but also cable strength. If these stress variations are added to those due to cable extension, total cable stress variation is obtained and resulting values are still small but relevant as shown on figure 13. According to this diagram, the maximum cable stress variation (difference between the maximum and minimum values) would be $18+10=28$ MPa while the maximum value obtained from the static analysis for this particular case was 17 MPa

Total cable stress variation due to cable extension and rotation at deck anchorage

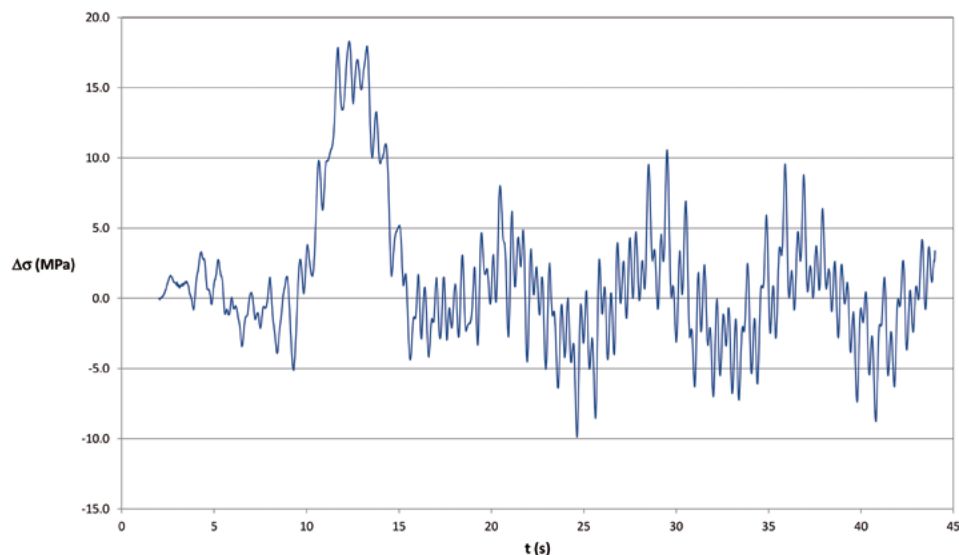


Figure 13. Total stress variation at the deck anchorage of the longest cable when the vehicle 3 of FLM2 (630 kN) runs through the cable-stayed bridge with a concrete deck and a 300 m long span at 100 km/h.

(data implicit in figure 5). Then the increment of the corresponding dynamic amplification factor after taking into account all the circumstances is $28/17=1.65$, which is well over the dynamic allowance which has been foreseen in the Eurocode.

In any case it has to be taken into account that the vehicle which has been considered in the analyses is the 630 kN vehicle of the FLM2 fatigue model which is quite exceptional and it already includes a dynamic allowance; from the point of view of fatigue, it would be necessary to consider all the vehicles corresponding to normal traffic (fatigue load models FLM4 or FLM5 are more appropriate) and results in terms of stress variations would be less relevant.

A similar analysis might be performed with respect to wind with similar results. The analysis should include buffeting effects to take into account the contribution of higher modes in the response of the bridge in order to activate possible parametric excitation of the cables.

A more rigorous analysis of this problem can only be performed on a particular case to take into account all the cables and all vehicle velocities to search for possible resonant effects. The example which has been shown here only considers non resonant effects for one cable and for one vehicle velocity. The response of the cable under resonance conditions (or even approaching resonance) may be completely different. What this analysis has shown is the fact that cable dynamics is a subject which has to be considered as one of the elements of design. It must also be pointed out that most cables which are being installed nowadays are provided with dampers and the resulting cable oscillations are very significantly reduced.

3.4. Aerodynamic effects due to service loads

Although no information has been published about aerodynamic effects due to service loads, these effects exist and they were detected during the monitoring and inspection of the

Sancho el Mayor cable-stayed bridge in Spain¹. This effect, which is obviously proportional to the square of the vehicle velocity, may be very important in the design of noise barriers for high speed trains and this is the reason why it is treated in the codes on railroad bridges [9]. As it also depends very much on the distance between the vehicle and the lateral structures (in this case, the cables), a reasonable minimum distance if there are no shoulders in the carriageway would be 1.75 m (half the width of the usual 3.5m lanes) plus the minimum safety distance between the traffic and the cables which is usually taken as 1.25 m (by today standards). Then the minimum distance between the vehicle axis and the cables would be 3.0 m. Consequently according to the Eurocode 1 [9], the basic pressure to be applied on the cables would be 0.12 kN/m^2 on a uniform vertical wall, or, in the case of the cables (with a drag coefficient of 0.8), 0.1 kN/m^2 if the vehicle velocity is 100 km/h. Then the scheme of pressures to be applied to the cables is as shown on figure 14.

Again in this case the longest cables are prone to experience the largest rotations at the deck anchorage so these are the cables to be checked. For so doing, the same model of the cable which was built to study parametric excitation (figure 10) is to be used for studying aerodynamic pressure from service loads. Only a few cases have been studied since this effect is not really important. These cases include short span bridges since the proportion of cable length being loaded is the highest and the longest span since a long cable may be prone to larger rotations at anchorages. Results are summarized on table 2. This table shows that the resultant stress variations are non-relevant in terms of fatigue for all cases. In actual bridges resultant stress variations may be larger because the distance between the vehicles and the cables may be significantly smaller but it

¹ The inspection and monitoring were carried out by the late Eng. Luis Ortega and the author. Results were not published.

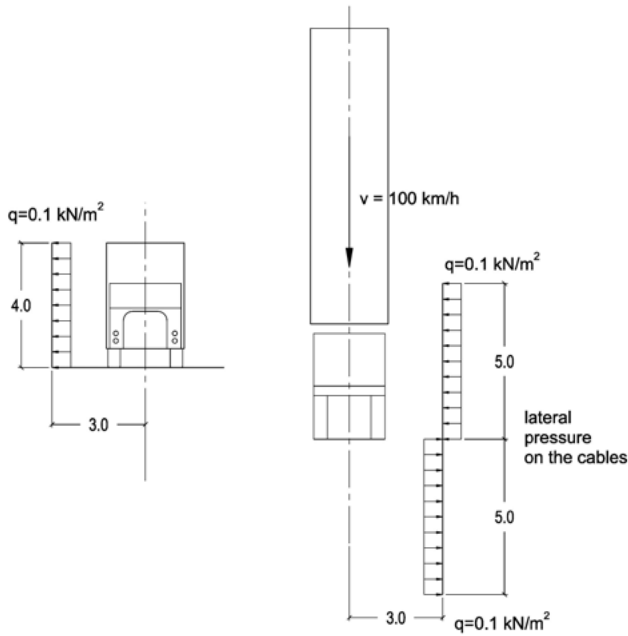


Figure 14. Pressure on cables for a heavy vehicle travelling at 100 km/h.

appears that, if the bridge is being designed according to current standards, aerodynamic pressure from traffic should not produce fatigue.

Table 2. Maximum stress variation in longest cable due to lateral aerodynamic pressure

Case	$\Delta\sigma = \sigma_{\max} - \sigma_{\min}$ (MPa)
Cable-stayed bridge with concrete deck – L=200 m	0.20
Cable-stayed bridge with concrete deck – L=300 m	0.34
Cable-stayed bridge with composite deck – L=600 m	0.89
Extradosed bridge with concrete deck – L=100 m	0.24

4. FATIGUE DUE TO WIND LOAD

As fatigue is the only concern of this study, the only wind effects which are to be considered are vortex shedding and buffeting. Galloping should in some cases be a matter of concern but only in those areas where ice forming in the cables is frequent. Wake galloping is also a phenomenon which has been observed in some bridges when the cables are organized in two close parallel vertical planes; as this is already a relatively well known effect, it may be avoided by different means. The case of rain-wind vibrations is somewhat similar although it is not yet fully understood; but the use of spiral strakes or protrusions or spherical dimples in the sheaths and dampers at the anchorages seems to have solved the problem in modern bridges. Then only the two previously mentioned phenomena are to be considered in this study.

4.1. Vortex shedding at the cables

Bridge vibrations due to wind flow vortex shedding are a matter of concern among bridge designers either in relation to

safety [31] or to comfort [32]. Nevertheless cable vibrations due to vortex shedding have been observed in some bridges [33] but they rarely are associated to fatigue problems. This is mainly due to the fact that critical wind velocities for the cables are very small and they should not cause relevant displacements in the cables. Critical wind velocity, U_c , is given by the equation [34]:

$$U_c = \frac{fD}{S_i} \quad (4)$$

where f is the cable frequency, D is the diameter and S_i is the Strouhal number whose value for a circular section is 0.18 [35]. As the range of fundamental frequencies for the cables ranges between 0.5 and 5 Hz (figure 3) and the mean diameter of the cables is 0.25 m, the range of critical velocities ranges between 0.7 m/s for the longest cables and 7 m/s for the shortest cables. These velocities should not cause important displacements in the cables. In the case of extradosed bridges fundamental frequencies for the shortest cables may increase up to 14 Hz and the corresponding critical velocity may reach 19 m/s which is a very relevant value; nevertheless this value corresponds to 15 m long cables, which should not be affected by vortex-shedding.

Nevertheless as vortex shedding vibrations actually happen, the cable deformation should be due to the development of higher vibration modes [33]. The study of such vibrations may be performed by applying the resonance model [33, 35, 36]. This methodology has given satisfactory results when comparing them to experimental values as shown on figure 15, corresponding to one cable of the River Suir Bridge in Ireland [33] (these cables were not equipped with external dampers). This figure shows that measured accelerations increase with wind velocity (it is especially relevant to observe results for wind velocities ranging from 10 to 15 m/s, which are far from the critical velocity corresponding to mode 1).

To study possible fatigue damage in the cables as a consequence of vortex shedding vibrations the same methodology may be applied. In a first stage and for a given cable, the maximum response for any given wind velocity is determined in terms of cable rotation at the anchorages. Then cable rotations are converted into stress variations by applying equation (3). For so doing it is determinant to define a value for damping ratio; if no dampers are provided a value of 0.1% (equivalent to 0.6% logarithmic decrement) should be applied; nowadays, as dampers are almost mandatory, a minimum value of 0.5% has to be applied although most suppliers claim they provide up to 2% damping; a value of 1% (equivalent to 6% logarithmic decrement) shall be used in this study. This value should increase for the longest cables as we will see that wind effects increase with cable length. The response is converted into cable stress by using equation (3). In a second stage Palmgren-Miner rule has to be applied once the statistical distribution of wind velocities and directions is known; alternatively, the Eurocode 1 [35] provides a simplified rule to avoid this computation.

Results are summarized in figure 16. All the points corresponding to every wind velocity have been plotted (there are 194 points for each velocity corresponding to all the cables for every one of the 12 bridges which are being considered). Then a continuous curve represents the envelope of all the results when the damping ratio of the cables is 1%; these max-

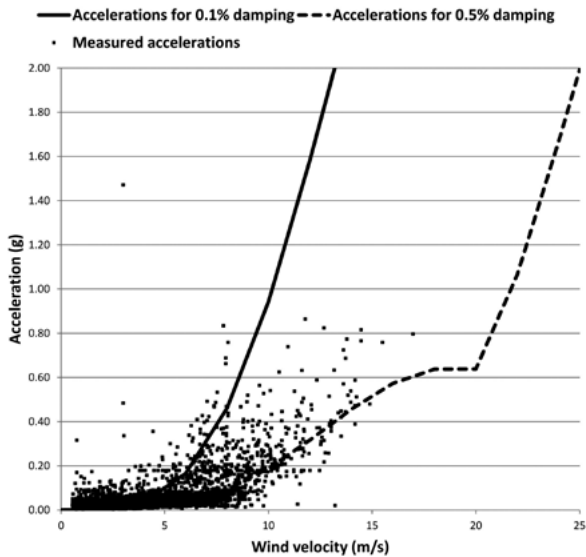


Figure 15. Measured and computed maximum accelerations at cable 16 of the River Suir bridge in Ireland [33].

imum values for each velocity generally correspond to the cable-stayed bridges with composite deck although they do not necessarily correspond to the longest cables nor to the longest spans; this curve indicates that vortex shedding by itself produces stress variations which fall below the fatigue limit although a combination with the oscillations which are due to service loads would yield larger values and might induce fatigue. Simultaneously a second curve has been drawn to represent the envelope of the results which would be obtained if damping ratio was reduced to 0.1% (a realistic value if anchorage dampers are not installed); in this case the stress variations may be larger than the fatigue limit and they could induce fatigue problems in the cables. In any case it must be taken into account that wind velocity very rarely exceeds 15 m/s (as

it may be observed in figure 15, which shows experimental values taken along more than one year) and the values shown on figure 16 for 0.1% damping are not as alarming as one could think from a fatigue point of view.

4.2. Buffeting at the cables

Sustained wind loads result in a relatively uniform pressure on the cables which is counteracted by a transverse sag and, consequently, by some cable rotations at the anchorages. These rotations would not be dangerous from the fatigue point of view if they were constant while wind is blowing (cycle counting would also be necessary after taking into account the frequency of wind storms). Nevertheless wind turbulence produces variations in the cable sag and, if the cables are long enough, wind may not be uniform along the full length of the cable and the resulting variable pressure yields some non-uniform transverse movement of the cables which may result in larger rotations and in a great number of loading cycles. The goal of this section is to give an oversight of the importance of this phenomenon in the overall behavior of the cables with respect to fatigue.

The response of the cables should depend on the turbulence characteristics of wind and the corresponding parameters depend on local conditions. Then it is necessary to assume some mean values of wind parameters: turbulence intensity shall be 0.15 and the mean height of cables with respect to ground has been assumed to be 60 m. The resulting integral scales of turbulence are derived as proposed by Strommen [37]. A wind history is digitally simulated [38] for a mean wind velocity of 20 m/s according to these parameters and the corresponding pressures are applied on the cable models which were presented before (figure 10). Two values of structural damping have been considered (0.1% and 1%) corresponding approximately to the cases where external dampers are applied to the cables or not. Aerodynamic damping has

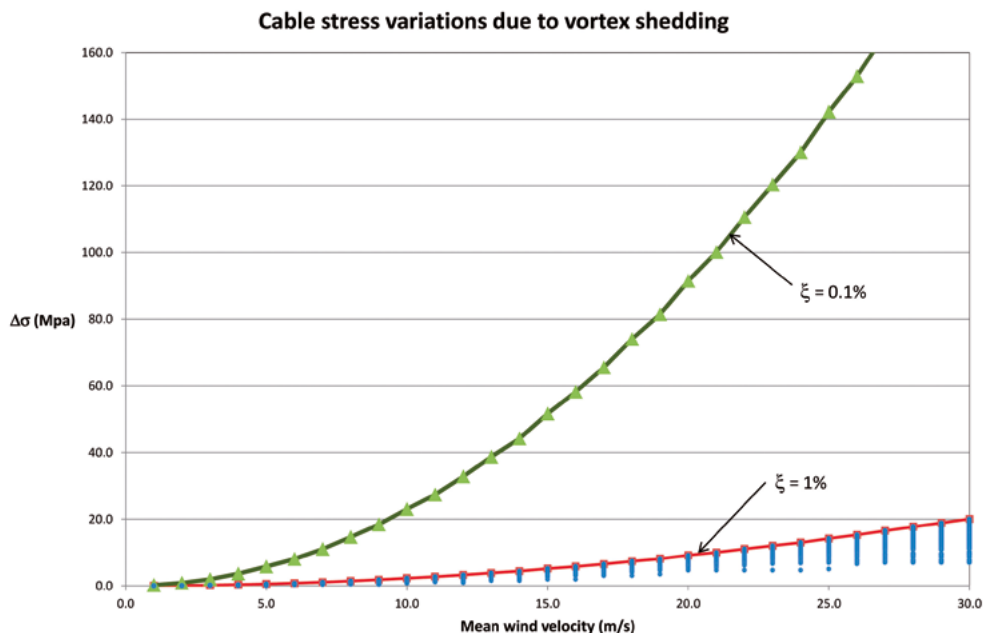


Figure 16. Cable stress variations due to vortex shedding at the cables for all the bridge solutions being considered and for two values of relative damping.

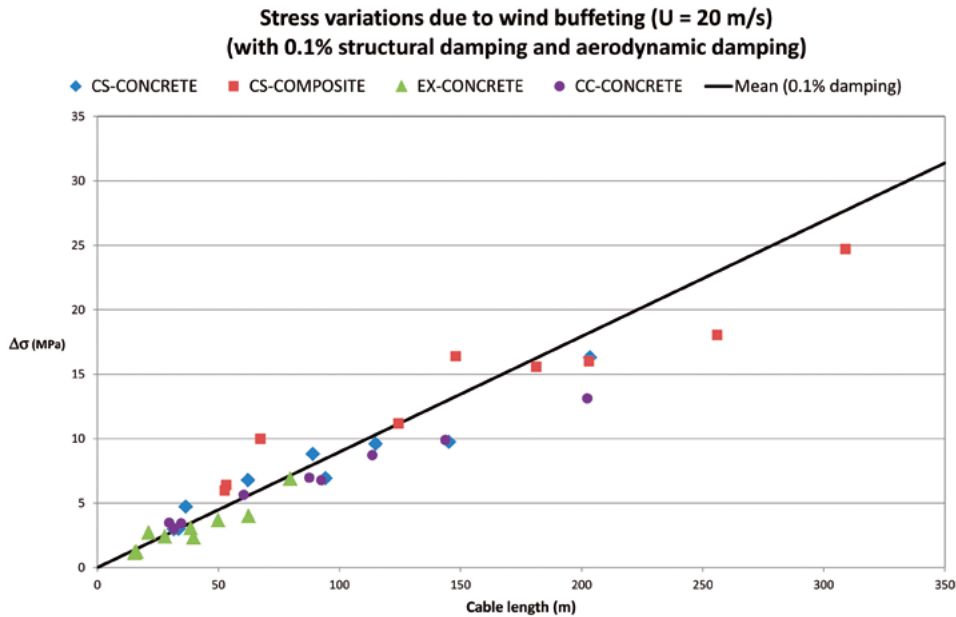


Figure 17. Stress variations in cables due to wind buffeting for a mean wind velocity of 20 m/s (0.1% structural damping and aerodynamic damping).

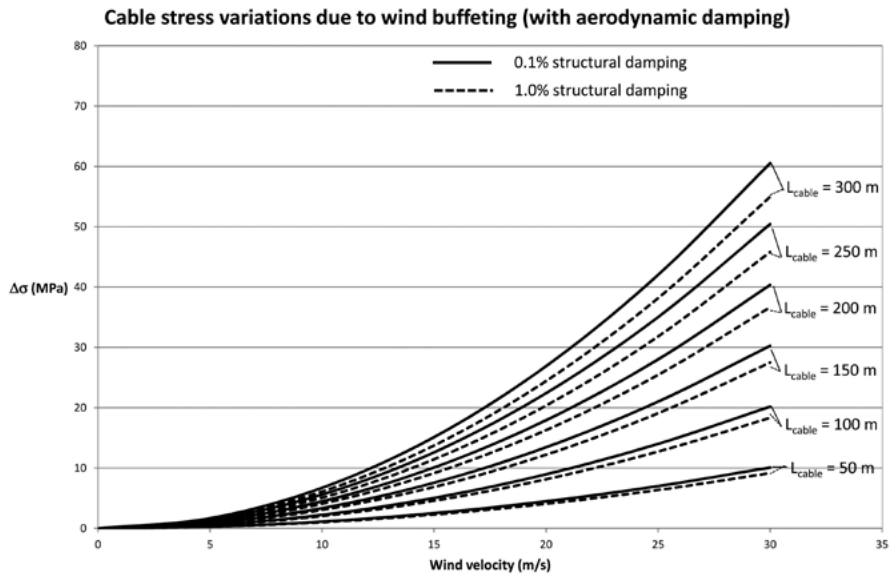


Figure 18. Stress variations in the cables due to wind buffeting as a function of wind velocity.

been considered in all cases since it may have a greater influence on the results than structural damping. Only three cables per bridge class have been studied: the shortest, the longest and an intermediate cable. Results are summarized on [figure 17](#) for a structural damping of 0.1% in the cables and the corresponding aerodynamic damping.

This figure shows that cable length is the governing parameter in the definition of stress variations. Composite bridges seem to yield slightly larger values and this is due to the fact that the permanent force in the cables is generally smaller than for concrete bridges. If a mean regression line is computed from these results and this relation is applied to different wind velocities the diagram of [figure 18](#) is obtained where the stress variations are plotted against wind velocity. This diagram allows an evaluation of the importance of wind buffet-

ing as a factor inducing fatigue. Stress variations for relatively frequent wind velocities (10 to 15 m/s) are smaller than 20 MPa, which is neatly smaller than the fatigue limit. The same calculations have been executed for two values of structural cable damping (0.1% and 1%) with smaller differences as compared to the results of vortex shedding; this due to the fact that the response to vortex shedding is resonant and then it is inversely proportional to damping while for buffeting the response corresponds to a variable force and this response is just slightly conditioned by damping. The values which have been obtained allow concluding that wind buffeting by itself may not induce fatigue. But again, it should be kept in mind that in this case the number of cycles is enormous during a wind storm and that these effects may be superposed to other effects which have been presented before.

Table 3.
Summary of stress variations in the cables of cable-stayed bridges

Fatigue source	CS-CONCRETE $\Delta\sigma$ (MPa)	CS-COMPOSITE $\Delta\sigma$ (MPa)	EX-CONCRETE $\Delta\sigma$ (MPa)	CC-CONCRETE $\Delta\sigma$ (MPa)
FLM1 (static)	23.4 - 77.4	42.0 - 86.4	21.8 - 87.8	23.7 - 45.4
FLM2 (static)	11.7 - 53.2	16.4 - 56.7	10.5 - 53.0	5.8 - 11.4
FLM3 (static)	11.5 - 53.7	16.3 - 55.4	9.4 - 50.5	5.7 - 11.2
FLM2 (dynamic, smooth) (mean increment with respect to static)	+38%	+21%	+30%	+13%
FLM2 (dynamic, rough) (mean increment with respect to static)	+101%	+50%	+185%	+31%
FLM2 (parametric excitation)(maximum increment found with respect to static)	+65%			
Aerodynamic lateral pressure (maximum values found in particular examples)	0.3	0.9	0.2	not checked
Vortex shedding (maximum values for any category)	For v=10 m/s: 23.0 MPa ($\xi=0.1\%$) and 2.3 MPa ($\xi=1\%$) For v=20 m/s: 91.5 MPa ($\xi=0.1\%$) and 9.2 MPa ($\xi=1\%$)			
Wind buffeting for 150 m long cables	For v=10 m/s: 3.4 MPa ($\xi = 0.1\%$) and 3.0 MPa ($\xi = 1\%$) For v=20 m/s: 13.4 MPa ($\xi = 0.1\%$) and 12.2 MPa ($\xi = 1\%$)			
Wind buffeting for 300 m long cables	For v=10 m/s: 6.7 MPa ($\xi\omega = 0.1\%$) and 6.1 MPa ($\xi = 1\%$) For v=20 m/s: 26.9 MPa ($\xi = 0.1\%$) and 24.4 MPa ($\xi = 1\%$)			

5. CONCLUSIONS

Fatigue conditions have been studied for the cables of cable-stayed bridges and extradosed bridges. Present methodology to check fatigue safety is based on the application of a number of fatigue load models which incorporate a dynamic allowance. According to the results which have been obtained for a wide range of bridges fatigue is generally not governing the design of the cables for highway bridges. The same may not be applicable to railroad bridges as it has been shown elsewhere [39].

As many potential causes for fatigue in the cables have been studied along this paper, a summary of relevant numerical values has been prepared (table 3) in order to compare the relative importance of these factors. This table only shows the minimum and maximum stress variations in each category.

The present study has shown that the dynamic allowance which is implicit in the definition of fatigue load models of the Eurocode may not be sufficient to check for fatigue. Dynamic stress variations in the cables due to the movement of the loads and to the roughness of pavement have been found to be relevant as compared to the stress variations obtained through a static analysis. In the cases where the cables are anchored at the deck axis, the influence of dynamic analysis and pavement roughness seems to be minor, mainly due to the fact that the fatigue loads are applied on the outside lanes (far from the cables) and these loads are shared by a greater number of cable stays.

In any case, the results relative to live loads and their dynamic effects show that it would be interesting to incorporate into the design methodologies a more precise description of service loads in order to allow a detailed check of actual stress oscillations (real or majored loads, number of cycles, effect of pavement roughness). This can only be done after a rigorous campaign of cable stress variations in monitored bridges. Present research has shown that these effects are relevant but the knowledge which is available to designers is not sufficient to undergo reliable alternative design methodologies. Future

structural codes should provide more precise descriptions of service loads in order to allow fatigue analyses taking into account dynamic effects and cycle counting. Present PTI method [14] is a good step forward although still very rough.

Parametric excitation and aerodynamic pressure from traffic have been found to yield very small stress variations. In the case of parametric excitation these conclusions apply to the range of bridges which has been considered but it may happen that in a particular bridge this phenomenon could be relevant. The recommended methodology to study parametric excitation has been presented.

Aeroelastic effects have been found to yield relatively small stress variations but they are relevant since they happen very frequently and they may be superposed to significant loads from traffic. Then it would be worthwhile to study possible conjunction between traffic, vortex shedding and buffeting. The presence of cable dampers reduces very significantly the stress variations due to vortex shedding effects while wind buffeting effects have been shown to be relatively independent of the cable damping.

Another idea which comes out as a conclusion of this research is the fact that a certain number of improvements of cable systems such as the presence of concentrators, dampers, patterned sheath surfaces or helical strakes have an obvious positive influence in the fatigue behaviour of cable stays and they have an almost null effect in the present design rules. This research has shown that a more rigorous analysis of cable stress variations would take into account these improvements and would result in positive effects for this technology.

Present design rules for cables are mainly based on limiting the axial stress in the cables and comparing it with a small value with respect to the actual strength of the steel (the well known $0.45f_u$ criterion). This limits very much the stress amplitude range and reduces the risk for fatigue (this is the main reason for maintaining those small stress limits). These rules have been proved to be safe since almost no accidents have been reported on modern bridges. Then a possible increase of

these limits could be considered but such an increase would require the consideration of all the effects which have been presented in this paper. This a goal which is worth to be investigated since it would end up in a reduction of materials quantities and, consequently, in more sustainable bridge designs.

Acknowledgement

The author is indebted to the late Eng. Luis Ortega Basagoiti for a lifelong friendship as well as for his comments on the importance of durability, repair and maintenance aspects in the design of bridges. We collaborated in the inspection and repair of several cable-stayed bridges and this paper is inspired by our discussions around this topic.

References

[1] Pipinato, A., Pellegrino, C., Fregno, G., Modena, C. (2012) Influence of Fatigue on Cable Arrangement in Cable-stayed Bridges, *International Journal of Steel Structures*, 12, 107-123, <https://doi.org/10.1007/s13296-012-1010-5>

[2] Otaola, J. (1982) Replacing Corroded Cables on a Cable-Stayed Bridge, *Civil Engineering—ASCE*, 52 (9), 78-80.

[3] Mehrabi, A.B., Ligozio, A. Ciolko, S.T. Wyatt, (2010) Evaluation, Rehabilitation Planning, and Stay-Cable Replacement Design for the Hale Boggs Bridge in Luling, Louisiana, *Journal of Bridge Engineering (ASCE)*, 15, [https://doi.org/10.1061/\(ASCE\)BE.1943-5592.0000061](https://doi.org/10.1061/(ASCE)BE.1943-5592.0000061)

[4] Sandberg, J., Hendy, C.R. (2010) Replacement of the stays on a major cable-stayed bridge, *Proceedings of the Institution of Civil Engineers - Bridge Engineering*, 163, 31-42, <https://doi.org/10.1680/bren.2010.163.1.031>

[5] Lavery, C., Moore, P., Vonk, E., Nagtegaal, G. (2013) Replacement of the Cable Stays at the Eijk Bridge, The Netherlands, *LABSE Symposium Report 99 (5)*, <https://doi.org/10.2749/222137813806548433>

[6] Dieng, L., Helbert, G., Chirani, S.A., Lecompte, T., Pilvin, P. (2013) Use of shape memory alloys damper device to mitigate vibration amplitudes of bridge cables, *Engineering Structures*, 56, 1547-1556, <https://doi.org/10.1016/j.engstruct.2013.07.018>

[7] Basu, S., Chi, M. (1981) Analytical Study for Highway Bridge Cables, *Federal Highway Administration, Report FHWA/RD-81/090*.

[8] Service d'études techniques des routes et autoroutes (SETRA), (2002) Cable stays Recommendations of French interministerial commission on Prestressing.

[9] European Committee for Standardization (2003) Eurocode 1: Actions on structures— Part 2: Traffic loads on bridges, EN 1991-2:2003.

[10] European Committee for Standardization (2005) Eurocode 3: Design of steel structures – Part 1.9: Fatigue, EN 1993-1-9:2005.

[11] European Committee for Standardization (2006) Eurocode 3: Design of steel structures – Part 1.11: Design of structures with tension components, EN 1993-1-11:2006.

[12] International Federation for Structural Concrete (fib) (2019) Acceptance of stay cable systems using prestressing steels, Bulletin 89, ISBN 978-2-88394-130-4.

[13] American Association of State Highway and Transportation Officials, AASHTO (2017) LRFD Bridge Design Specifications, 8th Edition.

[14] Post-Tensioning Institute (2018) Recommendations for Stay Cable Design, Testing and Installation, PTI DC45.1-18.

[15] Spanish Association for Structural Concrete (ACHE), (2007) Manual de tirantes, Colegio de Ingenieros de Caminos Canales y Puertos, ISBN: 9788438003534 (in Spanish).

[16] Wang, X., Wu, Z. (2011) Modal damping evaluation of hybrid FRP cables with smart dampers for long-span cable-stayed bridges, *Composite Structures*, 93, 1231-1238, <https://doi.org/10.1016/j.compstruct.2010.10.018>

[17] Xie, X., Li, X., Shen, Y. (2014) Static and Dynamic Characteristics of a Long-Span Cable-Stayed Bridge with CFRP Cables, *Materials*, 7, 4854-4877, <https://doi.org/10.3390/ma7064854>

[18] Yang, Y., Wang, X., Wu, Z. (2015) Experimental Study of Vibration Characteristics of FRP Cables for Long-Span Cable-Stayed Bridges, *Journal of Bridge Engineering (ASCE)*, 20, [https://doi.org/10.1061/\(ASCE\)BE.1943-5592.000656](https://doi.org/10.1061/(ASCE)BE.1943-5592.000656)

[19] Feng, B., Wang, X., Wu, Z. (2019) Fatigue life assessment of FRP cable for long span cable-stayed bridge, *Composite Structures*, 210, 159-166, <https://doi.org/10.1016/j.compstruct.2018.11.039>

[20] Svensson, H. (2012) *Cable-Stayed Bridges*, Ed. Ernst & Sohn.

[21] O'Brien, E.J., Rattigan, P., González, A., Dowling, J., Žnidarič, A. (2009) Characteristic dynamic traffic load effects in bridges, *Engineering Structures*, 31, 1607-1612, <https://doi.org/10.1016/j.engstruct.2009.02.013>

[22] O'Brien, E.J., González, A., Žnidarič, A. (2010) *Recommendations for dynamic allowance in bridge assessment, Bridge Maintenance, Safety, Management and Life-Cycle Optimization* – Frangopol, Sause & Kusko (eds), Taylor & Francis Group, London, ISBN 978-0-415-87786-2.

[23] Sanpaulesi, L., Croce, P. (2005) Design of Bridges, Leonardo da Vinci Pilot Project CZ/02/B/F/PP-134007.

[24] Oliva, J., Goicolea, J.M., Antolín, P., Astiz, M.A. (2013) Relevance of a complete road surface description in vehicle-bridge interaction dynamics, *Engineering Structures*, 56, 466-476, <https://doi.org/10.1016/j.engstruct.2013.05.029>

[25] Oliva, J., Goicolea, J.M., Astiz, M.A., Antolín, P. (2015) Fully three-dimensional vehicle dynamics over rough pavement, Proceedings of the Institution of Civil Engineers – Transport, 166, 144-157, <https://doi.org/10.1680/tran.11.00006>

[26] International Organization for Standardization (2016) Mechanical vibration – Road surface profiles – Reporting of measured data, ISO 8608:2016, <https://www.iso.org/standard/71202.html>

[27] Chen, N., Li, Y., Wang, B., Su, Y., Xiang, H. (2015) Effects of wind barrier on the safety of vehicles driven on bridges, *Journal of Wind Engineering and Industrial Aerodynamics*, 143, 113-127, <https://doi.org/10.1016/j.jweia.2015.04.021>

[28] O'Connor, C., Shaw, P.A (2000) *Bridge Loads*, Spon Press.

[29] Clément, H., Crémona, C. (1996) Étude mathématique du phénomène d'excitation paramétrique appliqué aux haubans de pont, Laboratoire Central des Ponts et Chaussées, OA 18.

[30] Caetano, E. (2009) Cable Vibrations in Cable-Stayed Bridges, *LABSE Bulletin SED 9*, Zurich.

[31] Astiz, M.A. (2010) Wind-induced vibrations of the Alconétar bridge, Spain, *Structural Engineering International*, 20, 195-199, <https://doi.org/10.2749/101686610791283696>

[32] Larsen, A., Poulin, S. (2005) Vortex-shedding excitation of box-girder bridges and mitigation, *Structural Engineering International*, 15, 258-263, <https://doi.org/10.2749/10168660577962919>

[33] Astiz, M.A. (2016) *Towards a standard policy for structural monitoring in cable-stayed bridges, Maintenance, Monitoring, Safety, Risk and Resilience of Bridges and Bridge Networks*, eds. T.N.Bittencourt, D.M.Frangopol, A. Beck, Taylor & Francis, 23-38, ISBN 9781138028517.

[34] Simiu, E., Scanlan, R.H. (1996) *Wind effects on structures : fundamentals and applications to design*, Wiley, ISBN: 0471121576.

[35] European Committee for Standardization (2005) Eurocode 1: Actions on structures – Part 1-4: General actions-Wind actions, EN 1991-1-4:2005.

[36] Ruscheweyh, H. (1980) *Wind induced vibrations of towers and stacks, Practical experiences with flow induced vibrations*, Eds. E. Naudascher & D. Rockwell D, 709-719, Springer (1980), ISBN: 3-540-10314-7.

[37] Strommen, E.N. (2010) *Theory of bridge aerodynamics*, Springer, ISBN: 3642448135.

[38] Cao, Y., Xiang, H., Zhou, Y. (2000) Simulation of stochastic wind velocity field on long-span bridges, *Journal of Engineering Mechanics (ASCE)*, 120, 1-6, doi: 10.1061/(ASCE)0733-9399126:1(1).

[39] Elices, M., Llorca, J., Astiz, M.A. (1994) *Fatigue of steels for concrete reinforcement and cables*, Handbook of Fatigue Crack Propagation in Metallic Structures, Ed.: A. Carpinteri, Elsevier, 191-220, ISBN: 978-0-444-81645-0.